Hydrol. Earth Syst. Sci. Discuss., 9, 5389–5436, 2012
www.hydrol-earth-syst-sci-discuss.net/9/5389/2012/
doi:10.5194/hessd-9-5389-2012

Hydrology and Earth System Sciences Discussions

Analysis of SMOS brightness temperature and vegetation optical depth data with coupled land surface and radiative transfer models in Southern Germany

F. Schlenz[1], J. T. dall'Amico[1], W. Mauser[1], and A. Loew[2]

[1]Department of Geography, University of Munich, Munich, Germany
[2]Max-Planck-Institute for Meteorology, KlimaCampus, Hamburg, Germany

Received: 10 April 2012 – Accepted: 11 April 2012 – Published: 20 April 2012

Correspondence to: F. Schlenz (f.schlenz@iggf.geo.uni-muenchen.de)

Published by Copernicus Publications on behalf of the European Geosciences Union.

Abstract

Soil Moisture and Ocean Salinity (SMOS) L1c brightness temperature and L2 optical depth data are analysed with a coupled land surface (PROMET) and radiative transfer model (L-MEB) that are used as tool for the analysis and validation of passive microwave satellite observations. The coupled models are validated with ground and airborne measurements under contrasting soil moisture, vegetation and temperature conditions during the SMOS Validation Campaign in May and June 2010 in the SMOS test site Upper Danube Catchment in Southern Germany with good results. The brightness temperature root-mean-squared errors are between 6 K and 9 K and can partly be attributed to a known bias in the airborne L-band measurements. The L-MEB parameterization is considered appropriate under local conditions even though it might possibly further be optimised. SMOS L1c brightness temperature data are processed and analysed in the Upper Danube Catchment using the coupled models in 2011 and during the SMOS Validation Campaign 2010 together with airborne L-band brightness temperature data. Only low to fair correlations are found for this comparison ($R < 0.5$). SMOS L1c brightness temperature data do not show the expected seasonal behaviour and are positively biased. It is concluded that RFI is responsible for most of the observed problems in the SMOS data products in the Upper Danube Catchment. This is consistent with the observed dry bias in the SMOS L2 soil moisture products which can also be related to RFI. It is confirmed that the brightness temperature data from the lower SMOS look angles are less reliable. This information could be used to improve the brightness temperature data filtering before the soil moisture retrieval. SMOS L2 optical depth values have been compared to modelled data and are not considered a reliable source of information about vegetation due to missing seasonal behaviour and a very high mean value. A fairly strong correlation between SMOS L2 soil moisture and optical depth was found ($R = 0.65$) even though the two variables are considered independent in the study area. The value of coupled models as a tool for the analysis

of passive microwave remote sensing data is demonstrated by extending this SMOS data analysis from a few days during a field campaign to a long term comparison.

1 Introduction

The European Space Agency's (ESA) Soil Moisture and Ocean Salinity (SMOS) mission was launched in November 2009 to monitor surface soil moisture and ocean salinity globally with a temporal resolution of 2–3 days and a spatial resolution in the order of 43 km (Kerr et al., 2010). Soil moisture is derived from multiangular interferometric passive microwave L-band brightness temperature measurements at 1.4 GHz and delivered on an ISEA (icosahedral Snyder equal area projection) grid with a mean distance between grid points of 12.5 km (Kerr et al., 2010). Potential applications of spaceborne soil moisture products are numerical weather forecasting, land surface hydrology, agricultural applications and climate research (Dirmeyer, 2000; Entekhabi et al., 1999; Bolten et al., 2010). An accuracy target of 0.04 $m^3 m^{-3}$ soil moisture random error is set for the SMOS L2 soil moisture measurements (Kerr et al., 2010; ESA, 2002). A central question for the validation of SMOS is whether and under which conditions this level of accuracy can be reached. This paper aims at contributing to answer this question.

It is important to validate remotely sensed soil moisture products properly in order to ensure good product quality that is a prerequisite for the application of the data. This is especially important as SMOS follows a novel technological concept. Validation of passive microwave soil moisture products is challenging due to the mismatch in scale between satellite products and point scale in situ measurements that are typically used for validation of remote sensing based soil moisture products (Bartalis et al., 2008; Prigent et al., 2005). In situ measurements for satellite validation are usually collected in field campaigns over extended areas and during short periods of time or over longer time spans at few selected measuring locations. In addition to other remote sensing data sets, the outputs of spatially distributed environmental process models can make a valuable contribution to the validation of remotely sensed soil moisture products (Crow et al., 2005; Albergel et al., 2010; Juglea et al., 2010; dall'Amico et al., 2012a). These data sets can help to extend long-term validation activities to larger areas.

Some studies have thoroughly evaluated the SMOS L2 products so far. The performance of the products behaves differently from region to region and changes with time (dall'Amico et al., 2012a; Albergel et al., 2012; Jackson et al., 2012; Gruhier et al., 2010; Parrens et al., 2012). Generally the SMOS performance in Central Europe seems to be degraded compared to other regions of the world. For the Upper Danube Catchment in Southern Germany, that is also the area of interest in this study, Albergel et al. (2012), dall'Amico et al. (2012a) and dall'Amico (2012) have compared SMOS L2 soil moisture products to in situ and modelled reference data. They find mean correlation coefficients of 0.25–0.3 and a dry bias in the order of 0.23 $m^3 m^{-3}$–0.267 $m^3 m^{-3}$ for the comparison of SMOS data with in situ data in 2010. For 2011 these figures improve considerably with a correlation coefficient of 0.52 and a dry bias of 0.15 $m^3 m^{-3}$ for the same comparisons (dall'Amico, 2012). In Europe the performance of the SMOS L2 soil moisture product was considerably affected by radio frequency interference (RFI) since the launch of SMOS (Albergel et al., 2012; Balling et al., 2011), but the amount of contaminated data has exhibited a decrease due to RFI mitigation efforts and switching off of RFI sources (Oliva et al., 2012). In 2010, several RFI sources were obvious in SMOS L1c data in Germany that have disappeared in 2011. Probably the improvement in SMOS performance in Southern Germany can at least partly be attributed to an improvement in the RFI situation.

Despite these improvements, the validation studies so far show that more work is still necessary to further improve the quality of the SMOS L2 soil moisture products in order to meet the mission target. Therefore it should be studied where the problems in the SMOS L2 soil moisture product originate from and how improvements could be achieved. Especially the pronounced dry bias in Germany and other regions needs further investigation. It needs to be clarified whether it is RFI-induced or has to do

HESSD
9, 5389–5436, 2012

with radiative transfer modelling uncertainties or other retrieval problems. Therefore it is essential to validate and study the radiative transfer modelling in the L-band of the microwave domain on the SMOS scale as SMOS soil moisture products are inverted through an iterative inversion method from L-band passive microwave observations (Kerr et al., 2010). The radiative transfer model used in the SMOS L2 soil moisture processor is the L-band Microwave Emission of the Biosphere (L-MEB) model (Wigneron et al., 2007) that serves as a forward model in the soil moisture inversion. Uncertainties in the parameterization of the radiative transfer model can result in errors in the retrieved variables (in most retrievals soil moisture and optical depth). As the L-MEB parameterizations used for the SMOS soil moisture retrieval have mostly been derived from studies with ground or airborne L-band radiometer measurements on the local scale it is possible that scaling issues introduce additional uncertainties. The vegetation optical depth, that is simultaneously retrieved with soil moisture and delivered in the SMOS L2 product, could be a valuable source of information about vegetation characteristics. However, Jackson et al. (2012) concludes that it does not contain reliable information in the US. This could point towards retrieval problems and should also be investigated in other parts of the world.

Few studies have validated and analysed the SMOS L1c products over vegetated surfaces which is important if the radiative transfer modelling abilities in the SMOS processing are to be studied. Examples are Albergel et al. (2011), Bircher et al. (2012), Montzka et al. (2011), Parrens et al. (2012). Albergel et al. (2011) and Parrens et al. (2012) have shown that there is still potential to improve soil moisture retrievals from SMOS brightness temperatures in Southern France. They used calibrated statistical relationships based on reference soil moisture values and additional information like leaf area index (LAI) simulated by a land surface model to produce better soil moisture estimates. Bircher et al. (2012) have compared SMOS L1c and airborne brightness temperatures with modelled brightness temperatures using in situ data as input on different spatial scales on one day in Denmark. They developed an improved L-MEB parameterisation for local conditions. Other studies rely either on ground based or airborne radiometer data as reference with the drawbacks of the mismatch in scale between radiometer and SMOS footprint. Also, airborne campaigns typically yield relatively small datasets of only a few days. With the help of coupled land surface and radiative transfer models these datasets can be extended beyond the typical scale and duration of field campaigns and thereby can serve as a valuable extension for SMOS validation and data analysis activities.

This study aims at assessing how coupled land surface and radiative transfer models can contribute to the validation and analysis of passive microwave remote sensing data. Possible explanations for the apparent problems in the SMOS L2 soil moisture data in Southern Germany are assessed. For this reason, SMOS L1c brightness temperature and L2 vegetation optical depth data are analysed with modelled and airborne data. If RFI would be responsible for most of the L2 problems this should be visible in the SMOS L1c brightness temperatures as well. And if SMOS L1c brightness temperatures would perform better than L2 data, this would point towards a problem in the soil moisture retrieval. Retrieved SMOS L2 optical depth values are analysed as they play an important role in the soil moisture retrieval and could be a valuable source of information about vegetation characteristics. Another important aspect is the parameterization of the radiative transfer model used for the soil moisture retrieval. It has been reported e.g. by Bircher et al. (2012) and Panciera et al. (2009) that it might be necessary to optimize the parameterization under local conditions to obtain best results. To study this, the radiative transfer modelling is analysed with airborne data as reference under local conditions. It has been reported that brightness temperatures at certain angles may be more reliable than at others (Bircher et al., 2012; Hornbuckle et al., 2011). Such a finding could also be exploited to improve the soil moisture retrieval by using only certain angular ranges. It is not the intention of this paper to study SMOS L2 soil moisture data as this has thoroughly been done already by dall'Amico et al. (2012a) and dall'Amico (2012).

The study is conducted in the highly instrumented Vils test site in the Upper Danube Catchment in Southern Germany that has been used as a major SMOS cal/val test site since 2007 (Delwart et al., 2008). Different extensive field campaigns have taken place here that produced time series of soil moisture station measurements. They are publicly available over the International Soil Moisture Network (ISMN) (Dorigo et al., 2011) http://www.ipf.tuwien.ac.at/insitu/. In addition to that ground based L-band radiometer measurements and spatially distributed data sets of soil moisture, vegetation and airborne L-band radiometer measurements are available (Schlenz et al., 2012a, b; dall'Amico et al., 2012b). The land surface model PROMET (Mauser and Bach, 2009) has been coupled to the radiative transfer model L-MEB to model land surface states in the Upper Danube Catchment on a 1 km grid as well as the resulting microwave emissions in the L-band. The coupled model is used as a tool for the analysis of the SMOS passive microwave satellite observations. As the SMOS data perform considerably better in 2011 than in 2010 the study concentrates on 2011 data. In addition to 2011 data, data from the SMOS Validation campaign 2010 are used for model validation and a brief SMOS data analysis as this is the only period with extensive ground and airborne data available.

In Sect. 2 the study area and data sets as well as the models involved in this study are described. This is followed by the description of the methodology. Section 3 details and discusses the results of the model validation, followed by an analysis of the radiative transfer model parameterization under local conditions on the SMOS scale with airborne brightness temperatures from the SMOS Validation campaign 2010. Next, SMOS L1c brightness temperature data are analysed and compared with the airborne brightness temperatures from the SMOS Validation Campaign 2010 in this period. Afterwards a long term comparison with modelled brightness temperatures from April to October 2011 is performed. SMOS L2 optical depth is compared against model results and the SMOS L2 soil moisture product before the main findings are summarized in the Conclusions.

2 Material and methods

The flowchart in Fig. 1 illustrates the context of the different data sets and comparisons in this paper. The coupled models PROMET and L-MEB produce data sets (black) of soil moisture (SM), vegetation optical depth (Tau), and brightness temperatures (BT) that are compared to SMOS data (red). In situ soil moisture (green) and airborne brightness temperatures (blue) are used for model validation. Additional comparisons of airborne brightness temperatures with SMOS L1c brightness temperatures and SMOS L2 soil moisture and optical depth values are also carried out.

2.1 Study area and in situ data

The study area is the Vils test site in the SMOS test site Upper Danube Catchment in Southern Germany. This region has been the subject of a wide range of hydrological, remote sensing and global change studies, e.g. Mauser and Schädlich (1998), Ludwig and Mauser (2000), Bach et al. (2003), Ludwig et al. (2003), Probeck et al. (2005), Loew et al. (2006), Mauser and Bach (2009). The Vils test site has roughly the size of a SMOS footprint and is situated in the northeast of the Upper Danube Catchment in an undulating terrain that is used agriculturally. It has a temperate humid climate and is considered homogenous with respect to terrain and land cover. It does not contain large water bodies or cities. The three most important agricultural land cover types are winter wheat, maize and grass that cover more than 60 % of the area. Based on previous studies (Strasser et al., 1999; Bach and Mauser, 2003; Loew, 2008), this test site has carefully been chosen and used for SMOS calibration and validation (cal/val) studies since 2007 (Delwart et al., 2008). The test site has been instrumented with seven soil moisture profile stations that have been measuring between 2007 and 2011 and has been subject of extensive field campaigns, the most comprehensive one being the SMOS Validation Campaign from 17 May to 8 July 2010. Details of this campaign are given in dall'Amico et al. (2012b). During this field campaign airborne L-band radiometer measurements were performed together with more than 9000 soil moisture and comprehensive vegetation parameter measurements that were collected in five selected focus areas sized roughly 3 by 7 km and distributed throughout the test site. The analysis in this study concentrates on the ISEA grid point 2027099 that is located in the centre of the Vils test site and the furthest away from any open water bodies. Two neighbouring grid points in the Vils test site have the IDs 2026586 and 2026587. Due to the homogeneity of the Vils test site the in situ and airborne measurements from the field campaigns are considered to be representative for the whole Vils test site. From the soil moisture stations the hourly 5 cm measurements from all available probes have been averaged per station and are being used as reference in this study. Figure 2 gives an overview of the Vils test site.

2.2 Airborne data

During the SMOS Validation Campaign the airborne L-band radiometer EMIRAD 2 (owned by the technical University of Denmark, Skou et al., 2010) was flown on five days onboard the Skyvan aircraft over the Vils test site to measure brightness temperatures emitted by the land surface over a representative portion of a SMOS footprint around SMOS morning overpass time. EMIRAD is a thoroughly validated radiometer that has been used in a variety of studies and is therefore used as reference in this study. EMIRAD has an antenna system consisting of two Potter horns, one pointed nadir and one 40° aft and has a footprint size of about 1.5 km for the nadir antenna and 2 km for the 40° looking antenna for an average flight altitude of 2 km above ground. The data processing is described in (Schlenz et al., 2012a) and involved RFI filtering with RFI flags that were provided with the data and a threshold filtering. After processing the data were available for the two look angles 0° and 40° for vertical and horizontal polarization. A detailed description of the airborne campaign data set is given by (dall'Amico et al., 2012b). Contrasting soil moisture, temperature and vegetation conditions were observed in the course of the campaign (focus area mean values of soil moisture varied between 0.169 $m^3 m^{-3}$ and 0.392 $m^3 m^{-3}$, air temperatures during overflight were between 7 °C and 18 °C, vegetation heights ranged between 7 cm and

HESSD
9, 5389–5436, 2012

79 cm). For further comparisons the EMIRAD data were mapped onto the ISEA grid with the nearest neighbour method.

2.3 SMOS data

SMOS L1c and L2 data are delivered on the ISEA grid with a mean distance between grid points of about 12.5 km, although the data have a mean resolution in the order of 43 km (Kerr et al., 2010). SMOS L1c brightness temperatures are valid for the whole SMOS footprint, which actual size is dependent on the incidence angle and therefore changes from one observation to the other. The SMOS L2 soil moisture and optical depth products are only valid for the nominal land cover class (low vegetation) within the footprint for which the soil moisture retrieval is carried out. Details about the geometry and other properties of the data products can be found in the Algorithm Theoretical Basis Document (ATBD) of the SMOS L2 Soil Moisture Processor (Kerr et al., 2011). Only SMOS data from morning orbits (around 06:00 a.m. local time) are used to avoid uncertainties related to differences between morning and evening overpasses that have been found by (Rowlandson et al., 2012).

In order to make the SMOS L1c data usable a comprehensive data processing chain has been developed and set up that helps to reduce the noise in the data and makes it easier to interpret. The processing consists of filtering, geometric and Faraday rotation and an incidence angle based analysis. The processing has been adapted from the official SMOS L2 soil moisture processing described in Kerr et al. (2011). In a first step observations that are RFI flagged or do not fulfil the spatial resolution requirements because the footprint is too large or elongated are filtered out by applying:

$$\frac{\text{axis1}}{\text{axis2}} > 1.5 \quad (1)$$

and

$$\sqrt{4 \cdot \text{axis1} \cdot \text{axis2}} > 3025 \quad (2)$$

HESSD
9, 5389–5436, 2012

where axis1 and axis2 are the half lengths of the major and minor axis of the 3 dB contour of the near elliptical SMOS footprint. Afterwards, several RFI filtering techniques are performed to detect strong RFI. These include a threshold filtering deleting all brightness temperatures above 300 K and below 200 K as only land surfaces are considered, the upper and lower thresholds for the imaginary part of full polarized brightness temperatures are −50 K and 50 K, respectively. Another test compares the amplitudes of the brightness temperatures to its expected range with:

$$50 < \sqrt{\mathrm{TB}_X^2 + \mathrm{TB}_Y^2} < 500 \tag{3}$$

and filters out data exceeding these thresholds. Additional techniques are applied to filter for soft RFI. These are based on the fourth Stokes parameter ST4 that is required to be below the threshold of 50 K and the mean value of the halved first Stokes parameter of all observations for one pixel $\langle \mathrm{TBS1} \rangle = 0.5 * (\mathrm{TB}_X + \mathrm{TB}_Y)$. Following condition needs to be fulfilled to pass the test for brightness temperature observations:

$$\left(\mathrm{TBS1} - \langle \mathrm{TBS1} \rangle\right) > 5.0 + 4.0 \cdot \mathrm{DTB}_X \tag{4}$$

where DTB_X is the radiometric uncertainty related to TB_X. This test is only reasonable in homogenous areas where brightness temperature variations within one pixel do not arise from a large surface heterogeneity (e.g. coastlines). Most of these threshold have been taken from Kerr et al. (2011) while some are more strict than the values used in the SMOS L2 processing. They have been tested with airborne and SMOS brightness temperatures and proven to be valuable under local conditions.

L1c data are delivered as top of atmosphere (TOA) brightness temperatures in antenna geometry that need to be rotated to enable a comparison with brightness temperatures on the Earth's surface which is performed in the next step. The necessary rotations comprise a geometric rotation to correct for the transformation from antenna to Earth surface reference frame and the Faraday rotation to correct for the influence of the atmosphere on the brightness temperatures. The rotations are detailed in Kerr

HESSD
9, 5389–5436, 2012

et al. (2011). After the rotations, the vertical and horizontal polarized brightness temperatures are averaged into 10° bins that are centred around the designated angle to enable an incidence angle based analysis. A similar approach was chosen by Parrens et al. (2012).

This processing reduces the noise in the data considerably but outliers that are probably related to RFI are still present in the data.

The SMOS L2 optical depth data have been processed analogue to the SMOS L2 soil moisture processing as described in dall'Amico et al. (2012a). It involves a filtering using the DQX value and the flags FL_NO_PROD, FL_RFI_Prone_H, FL_RFI_Prone_V and FL_RAIN (Kerr et al., 2011). This processing reduces noise in the data by deleting some outliers with suspicious data but there are still outliers left in the data that are probably connected to RFI that is not detected by the methods and flags used.

dall'Amico (2012) have thoroughly analysed the SMOS L2 soil moisture data for April to October 2011 in the Vils test site with in situ data and PROMET simulations. They find correlation coefficients for the comparison between SMOS and in situ soil moisture in the Vils test site of around 0.52 and a dry bias of around 0.15 $m^3 m^{-3}$. For comparisons between modelled soil moisture and SMOS soil moisture the mean correlation coefficient in the Vils test site for 2011 is 0.54, the mean bias 0.13 $m^3 m^{-3}$.

2.4 Coupled land surface and radiative transfer modelling

The hydrological land surface model PROMET (PROcesses of Mass and Energy Transfer, Mauser and Bach, 2009) and the microwave emission model L-MEB (L-band emission of the biosphere, Wigneron et al., 2007) have been coupled to model land surface states (e.g. soil moisture, temperatures, vegetation parameters) and the resulting microwave emission to validate and analyse SMOS L1c brightness temperatures as well as SMOS L2 optical depth data. Two publications have already validated the models and discussed the uncertainties related to this modelling approach thoroughly. While Schlenz et al. (2012a) have focussed on the validation and uncertainties related to the land surface modelling from point to SMOS-like scale in the Upper Danube Catchment

HESSD
9, 5389–5436, 2012

and brightness temperature modelling on the SMOS-like scale in the Vils test site, Schlenz et al. (2012b) have analysed the radiative transfer modelling on the point scale in a test site roughly 100 km southwest of the Vils test site. Therefore it is referred to these publications for a more thorough discussion of the related uncertainties.

2.4.1 Land surface model PROMET

In the present study the hydrological land surface model PROMET is used to simulate fields of land surface states with an hourly resolution on a 1 km grid in the Upper Danube Catchment. A detailed description of the model physics is given by Mauser and Bach (2009) and Mauser and Schädlich (1998). The model describes all relevant water and energy fluxes related to the radiation balance, vegetation, soil, snow, and land-surface-atmosphere exchange processes. It is spatially distributed and based on high resolution spatial input data like land cover and soil maps and meteorological forcing data from station networks or regional climate models as input. In our case the meteorological station network delivering the meteorological forcing consists of more than 130 stations operated by the Bavarian State Research Center for Agriculture. The land cover map has been derived from high resolution satellite imagery and statistical information on community level, the soil map is taken from a combination of the European and German soil map and regional soil information supplied by the (BÜK, 1997). The soil moisture dynamics modelling is done in PROMET with a 4-layer soil model based on an explicit solution of the Richards equation for flow in unsaturated media (Philip, 1957) while the soil water retention model of (Brooks and Corey, 1964) is used to relate soil suction head to soil moisture content. The 4 soil compartments were selected to be situated at 0–2, 2–15, 15–50 and 50–150 cm depth for this study. For all comparisons between modelled and measured soil moisture the second soil layer is used, as its depth corresponds to the depth where most soil moisture measurements were performed. The average of the first two layers is used for brightness temperature modelling and SMOS comparisons as the penetration depth of microwaves in the L-band is typically 5 cm (Kerr et al., 2010). The model has been validated in different

HESSD
9, 5389–5436, 2012

test sites on different scales with good results by Mauser and Schädlich (1998), Ludwig and Mauser (2000), Mauser and Bach (2009), Loew et al. (2006), Strasser and Mauser (2001), Pauwels et al. (2008). Muerth (2008) evaluated the soil temperature modelling abilities of PROMET in the Upper Danube Catchment with measurements and remote sensing data with good results.

For the analysis of the 2011 data set the dynamic vegetation model within PROMET was used. It models the vegetation development dynamically depending on the soil and weather characteristics for all individual pixels. Plant development is simulated with a 2 layer canopy model, which iteratively closes the energy balance for the sub canopy soil surface and each layer of the canopy and thereby produces a canopy radiation temperature. Details are given in Hank (2008). The modelled vegetation parameters phenology, vegetation height, vegetation biomass and leaf area index (LAI) of this model, which evolve dynamically accoding to the course of the weather, have been compared to ground measurements with very good results by Hank (2008) in the centre of the Upper Danube Catchment for several test sites on wheat, oat, maize and grassland during several years. (Hank, 2008) assessed e.g. the modelled LAI with a mean R^2 of 0.925 (0.92) and a mean Nash-Sutcliffe coefficient of 0.83 (0.87) for wheat (maize).

Schlenz et al. (2012a) have compared modelled soil moisture from PROMET with soil moisture measurements on different scales. The measurements were conducted on the local scale at nine soil moisture measuring stations in and around the Vils test site that have been measuring between November 2007 and November 2010 and on the regional scale with handheld probes during the SMOS Validation Campaign 2010 on 8 days between May and July 2010 in an area considered representative for the central SMOS grid point in the Vils test site (Schlenz et al., 2012a). They concluded that the uncertainties of the soil moisture modelling decrease from local to regional scale with a mean root-mean-squared error (RMSE) of 0.094 $m^3 m^{-3}$ on the local scale and 0.040 $m^3 m^{-3}$ on the regional scale. The mean R^2 on the local scale is 0.60. A bias leads to high RMSE values especially in wet conditions which leads to an underestimation in the reproduction of the seasonal soil moisture dynamics through PROMET.

HESSD
9, 5389–5436, 2012

A detailed analysis of the soil moisture modelling uncertainties described by Schlenz et al. (2012a) showed that four of the five stations with the highest RMSE values are located on the same soil type. As the laboratory soil texture analysis from soil samples taken at these stations differed substantially from the soil texture used in the model parameterization, that is derived from the Global Soil Data Base the soil parameterization was improved for this soil type based on the laboratory results of a soil texture analysis. This new parameterization in addition to other model improvements led to a clear reduction of the soil moisture modelling uncertainties. The mean RMSE of those four stations decreased from 0.122 $m^3 m^{-3}$ to 0.057 $m^3 m^{-3}$ while the mean R^2 increased from 0.52 to 0.70. Overall this new parameterization leads to a mean RMSE over all stations of 0.065 $m^3 m^{-3}$ and a mean R^2 of 0.71. Applied to the whole test site this new parameterization leads to a slightly improved RMSE of 0.039 $m^3 m^{-3}$ on the regional scale. Figure 3 shows the comparison of the modelled and measured 5 cm soil moisture mean of the five soil moisture stations that are within a 20 km radius around SMOS ID 2027099 for 2011. The deviations between both data sets are small.

Loew and Schlenz (2011) have used an extended version of the triple collocation method (Miralles et al., 2010) to assess relative soil moisture errors of PROMET, the in situ measurements from the stations in the UDC and coarse scale satellite soil moisture products. They conclude that the soil moisture random error of PROMET is better than 0.025 $m^3 m^{-3}$ on the SMOS scale which is consistent with similar findings of Schlenz et al. (2012a).

2.4.2 Radiative transfer model L-MEB

The microwave emission model L-MEB, which is also part of ESA's SMOS Level 2 soil moisture processor, is used to simulate L-band brightness temperatures from the continuous soil vegetation layer in the Upper Danube Catchment on a 1 km resolution. A comprehensive description of the model is given by Wigneron et al. (2007). This zero-order Tau (τ)–Omega (ω) radiative transfer model uses PROMET soil moisture, soil surface temperature and LAI fields as input for the modelling. The polarized

HESSD
9, 5389–5436, 2012

($p = h$, v) brightness temperature TB_P [K] is calculated through a sum of the three terms soil emission attenuated (scattered and absorbed) by the vegetation, direct vegetation emission and vegetation emission reflected by the soil and attenuated by the vegetation again:

$$TB_P = (1 - \omega_p)(1 - \gamma_p)(1 + \gamma_p r_{Gp}) T_C + (1 - r_{Gp}) \gamma_p T_G \tag{5}$$

where γ_p is the vegetation attenuation factor [–] and ω_p is the vegetation single scattering albedo [–]; T_G and T_C are the effective temperature of the ground and the canopy [K], respectively. r_{GP} is the reflectivity of the rough soil [–] which is typically described as a function of the Fresnel reflectivities of a smooth surface, modified by a surface component. The vegetation attenuation factor γ_p is described as a function of the vegetation optical depth τ at nadir and the observation angle. The effective temperature of the ground, T_G, is calculated from the surface and deep (50 cm) soil temperatures by the approach of Wigneron et al. (2007) and T_C is approximated by PROMET's air temperature. The vegetation optical depth is calculated using LAI values from PROMET with the approach of Wigneron et al. (2007). The optical depth of forests is fixed to a defined value. The roughness parameter H_R over grass is soil moisture dependent (Saleh et al., 2009).

The land cover specific L-MEB parameters used for the modelling are summarized in Table 1, they are in line with the parameters used by Wigneron et al. (2007); Saleh et al. (2007); Grant et al. (2007) and have been taken from a compilation of parameterisations of L-MEB based on experimental studies (J.-P. Wigneron, personal communication, 2012) that forms the basis of the SMOS L2 processor parameterisation. These parameters agree mostly with the default parameters that are being used in the operational version of the SMOS L2 processor for Central European Crops (Kerr et al., 2011). The rape parameterisation developed by Schlenz et al. (2012b) has been added.

As different authors have reported that it might be necessary to parameterize L-MEB locally to obtain optimal results (Panciera et al., 2009; Bircher et al., 2012), the radiative transfer modelling abilities of the coupled models PROMET and L-MEB have been validated on the local scale by Schlenz et al. (2012b) near Munich over a rape field and on the SMOS scale by Schlenz et al. (2012a) in the Vils test site. To test the suitability of the L-MEB parameters under local conditions (Schlenz et al., 2012a) have compared modelled brightness temperatures to airborne measurements of brightness temperatures from the airborne L-band radiometer EMIRAD (Skou et al., 2010) on basis of the SMOS ISEA grid for the look angles 0° and 40° for five days during the SMOS Validation Campaign 2010. They concluded that the model performs very well on three of the campaign days while on two days there are deviations between model results and measurements. RMSE values for this comparison at the central ISEA ID in the Vils test site (2027099) are 16.52 K and 13.14 K for horizontal and vertical polarization of the 40° look angle and 12.97 K and 12.09 K for horizontal and vertical polarization of the 0° look angle, respectively. Through the usage of the improved land surface model now using a dynamic vegetation model these error values have decreased substantially to 8.39 K and 8.98 K for horizontal and vertical polarization of the 40° look angle and 6.80 K and 6.45 K for the horizontal and vertical polarization of the 0° look angle, respectively. As EMIRAD is a reliable radiometer that has been thoroughly calibrated and used in a variety of studies it is used as reference here. These comparisons are thoroughly discussed in Sect. 3.1.

Schlenz et al. (2012b) have developed a new L-MEB parameterization for winter rape and tested the suitability of it for soil moisture retrievals from ground based multiangular L-band brightness temperature data of a ELBARA II radiometer (Schwank et al., 2009) situated in Puch near Munich in the Upper Danube Catchment. They also analysed the sensitivity of L-MEB to different parameterisations under local conditions. They conclude that the soil moisture retrieval with L-MEB works satisfyingly over rape and that the optical depth parameterisation and the roughness parameterisation are crucial for the radiative transfer modelling. These results are consistent with a variety of studies that stress the importance of correct optical depth and roughness parameterization for radiative transfer modelling, e.g. Bircher et al. (2012), Panciera et al. (2009).

For further comparisons the modelled brightness temperature data were mapped onto the ISEA grid with the nearest neighbour method.

2.5 SMOS L1c data analysis

After the performance of the L-MEB parameterization under local conditions has been analysed with a comparison between modelled and airborne brightness temperatures these airborne brightness temperatures are also compared to SMOS L1c data during the SMOS Validation Campaign 2010. Afterwards SMOS L1c data are compared to modelled brightness temperatures for a range of look angles for the year 2011.

2.5.1 Comparison with airborne brightness temperatures during the SMOS Validation Campaign 2010

During the SMOS Validation Campaign 2010 airborne brightness temperatures are available for the Vils test site from the EMIRAD radiometer for five days on which SMOS morning overpasses have taken place. Unfortunately only on two of those days SMOS L1c data with sufficient quality are available, and only on 17 June a value for the 0° look angle is available. Those data sets of EMIRAD and SMOS measurements are compared for the five campaign days at the central ISEA grid point in the Vils test site for the two EMIRAD look angles 0° and 40°. As Bircher et al. (2012) found out that neither using the EMIRAD antenna pattern nor the SMOS antenna pattern for weighting the brightness temperatures for a similar comparison between SMOS L1c, EMIRAD and modelled brightness temperatures improved the results over applying simple means, the same simplification was applied here. The results are presented in Sect. 3.2.1.

2.5.2 Comparison with modelled brightness temperatures in 2011

To enable a longterm analysis of SMOS L1c brightness temperatures under varying soil moisture and vegetation conditions, they are compared to modelled brightness temperatures in 2011 from April to October on the basis of the ISEA grid to which the model data have been mapped with the nearest neighbour approach. For the ISEA grid points in the Vils test site these comparisons are performed for the angles 10°, 20°, 30°, 40° and 50° for both polarizations. They are presented and discussed in Sect. 3.2.2.

2.6 SMOS optical depth analysis

To study whether the optical depth values in the SMOS L2 soil moisture product that are obtained during the soil moisture retrieval contain valuable information, they are compared to modelled values of optical depth using vegetation parameters from the dynamic vegetation model PROMET for 2011. The modelled values are mapped to the ISEA grid using the nearest neighbour method and the time series for every ISEA grid point is compared to SMOS optical depth values. To test whether there is a relation between retrieved SMOS L2 soil moisture and optical depth the correlation for both data sets for 2011 is calculated. The results for the ISEA IDs in the Vils test site are presented and discussed in Sect. 3.3.

3 Results and discussion

3.1 Model validation and L-MEB parameterization under local conditions

In Sect. 2.4.1 it is reported that the land surface model PROMET and specifically the soil moisture submodel has been validated extensively in different studies and works well in the Upper Danube Catchment and especially the Vils test site. A RMSE of $0.039\,m^3\,m^{-3}$ on the regional scale has been reported.

The radiative transfer modelling abilities under local conditions of the coupled models PROMET and L-MEB have been summarized in Sect. 2.4.2. To illustrate these results, Fig. 4 compares modelled brightness temperatures in the Vils test site on five days during the SMOS Validation Campaign 2010 with measurements from the airborne

HESSD
9, 5389–5436, 2012
Analysis of SMOS data with coupled models
F. Schlenz et al.

L-band radiometer EMIRAD for the 40° look angle. The error bars indicate the standard deviations from the averaging.

The vertically polarized brightness temperature shows a relatively constant offset in the order of 5–10 K while the horizontally polarized brightness temperature does not. This can partly be explained with a systematic bias of ~3.5 K that was observed for the EMIRAD 40° horizontal channel throughout the SMOS Validation Campaign 2010 as reported in Bircher et al. (2012). Since this only explains parts of the observed bias, other factors could also play a role here but due to the uncertainties related with the EMIRAD bias this issue is not further investigated. Possibly the L-MEB parameterisation could further be optimized. No systematic bias is observed for the 0° look angle (not shown), the RMSE is largely determined by deviations on the last day.

It is considered promising that on four of the five days the model works reliably despite contrasting soil moisture, temperature and vegetation conditions. This leads us to the overall conclusion that the coupled models work reliably and the parameterisations chosen for L-MEB are appropriate under the local conditions. Especially the roughness and vegetation optical depth parameterisation seem to be appropriate as the model performance does not change significantly during the first four days even though vegetation grows strongly during this time. For example, the mean vegetation height of all wheat fields in the focus areas increases from 40.2 cm to 77.9 cm during those four flight days. Growing vegetation increases the importance of correct vegetation parameterisation through an increase in vegetation optical depth. An incorrect soil roughness parameterisation would lead to a clear offset between model output and measurements in all angles and polarizations, especially at the beginning.

On the last day there is a considerable deviation between measurements and model output, that is also apparent for the 0° look angle (not shown). While the measured brightness temperatures decrease by about 15 K, the modelled vertically polarized brightness temperature decreases by only about 4 K and the horizontally polarized brightness temperature increases by about 5 K. It is not possible to give a simple explanation for this deviation between model output and measurements. Modelled soil moisture and temperatures do not show any abnormality (soil moisture deviations between model and field measurement for the whole Vils test site are below 0.03 $m^3 m^{-3}$ as for most of the other days, too). When compared to the earlier days the vegetation growth is considerably smaller between the last two days, all of the three most important plants wheat, maize and grass grow less than 8 cm on average in this time frame. A feature that is different on the last day in comparison to all other days is that the upper soil layer is very wet and that standing water is present in the area due to considerable precipitation events shortly before the EMIRAD overflight. This may be part of an explanation for the distinct behaviour of the brightness temperatures on this day. It is known that high soil moisture gradients in the upper soil layer, standing water and interception after precipitation events can lead to problems in the radiative transfer modelling which has also been reported by (Jackson et al., 2012; Rowlandson et al., 2012). Therefore the observed deviation does not necessarily point toward a parameterisation problem but should be further investigated. Overall the L-MEB parameterisation works very well under contrasting conditions and is considered appropriate under local conditions so that no further investigations on the parameterisation are performed. Yet, it is possible that the parameterisations could further be optimised under local conditions.

3.2 Analysis of SMOS L1c data

3.2.1 Comparison with airborne brightness temperatures during the SMOS Validation Campaign 2010

Figure 4 compares EMIRAD, SMOS and modelled brightness temperatures for the central ISEA grid point in the Vils test site for EMIRAD's 40° look angle at around 06:00 a.m. local time which corresponds to the SMOS morning overpass time. All 40° SMOS observations are larger than their EMIRAD counterpart while the 0° observation is lower. The RMSEs are 17.02 K and 28.05 K for the horizontal and vertical polarization of the 40° angle, respectively. For the 0° angle (not shown here) the RMSEs are 11.12 K and 11.55 K for the horizontal and vertical polarization, respectively. SMOS data show

HESSD
9, 5389–5436, 2012

the expected behaviour with vertically polarized brightness temperatures being higher than the horizontally polarized ones for 40° and both being essentially the same for 0°. But a RMSE between 11.12 K and 28.05 K can be considered a substantial deviation that may be attributed at least partly to RFI problems. Due to the small sample size this comparison is not considered reliable enough to draw further conclusions. Of course this comparison involves some approximations related to the different geometries of the two data sets. The SMOS L1c data are valid for a larger area than what is being mapped to each ISEA grid point in a nearest neighbour mapping approach. Hence the SMOS L1c data are valid for a larger area than the EMIRAD data. But as the Vils test site is very homogenous concerning soil, land cover, climate and topography it is assumed that this difference of geometries plays a very small role. In addition to that the centre of the SMOS footprint contributes more to the SMOS brightness temperature value than the edges due to the antenna pattern. This is being confirmed by the low variation of EMIRAD brightness temperatures of the neighbouring ISEA grid points. If a mean value of the three Vils ISEA grid points 2027099, 2026586 and 2026587 is calculated the deviation of this value from the 2027099 value never reaches 2 K. The homogeneity of the area is also the reason for the assumption that the EMIRAD data are representative for the whole area even though the EMIRAD flight lines do not cover the whole area. The flight pattern was planned carefully in order to best represent the variability present in the Vils test site.

3.2.2 Comparison with modelled brightness temperatures for the year 2011

To study SMOS L1c brightness temperatures in different seasons a long term comparison of SMOS L1c brightness temperature with modelled brightness temperatures has been performed for the central ISEA grid point for April to October 2011. The statistics for the analysis of modelled with SMOS L1c brightness temperatures are summarized in Table 2 for the look angles 10°, 20°, 30°, 40° and 50°.

It is apparent that the correlations between both data sets are only low to fair ($R < 0.45$) with RMSE values around 11–22 K. For horizontal polarization correlations

HESSD
9, 5389–5436, 2012

get better with increasing look angle, except for the 10° angle. The vertical polarization behaves similarly. These correlations are generally lower than the correlations between PROMET and SMOS L2 soil moisture which is 0.57 for the ID 2027099 in 2011 (dall'Amico, 2012). Concerning regressions and RMSE values the vertically polarized brightness temperatures perform better than the horizontally polarized ones. The bias for the horizontal polarization increases with increasing look angles. The regressions for the vertical polarization improve with increasing angles. Following radiative transfer theory, the horizontally polarized brightness temperatures are expected to decrease with increasing look angle, while the vertically polarized ones are expected to be generally higher and increase with increasing look angles. The expected behaviour is only observable for the vertically polarized observations.

In general the horizontally polarized brightness temperatures seem less reliable than the vertically polarized ones and the lower look angles perform inferior to the higher angles. One has to keep in mind that the significance of the results for the angles below 30° is lower due to the smaller sample size. The lower performance of SMOS data for the lower look angles is consistent with findings of Bircher et al. (2012) and may be related to the SMOS interferometric imaging technique.

As the correlations between SMOS L1c and modelled brightness temperatures are inferior to the correlations between SMOS L2 and modelled soil moisture, the problems in the SMOS L2 soil moisture product are considered to originate not primarily from a retrieval problem. A pure retrieval problem would mainly be visible in the L2 data, but not in L1c data, if the radiative transfer modelling works reliably. As it was shown in Sect. 3.1 that the radiative transfer modelling works reliably under most conditions in the study area, this points towards an RFI issue because it affects both L1c and L2 data. The mean positive bias in the SMOS brightness temperatures (compare Table 2) adds to this argumentation. Oliva et al. (2012) state that RFI can produce higher SMOS brightness temperatures which would lead to a dry bias in the soil moisture retrievals. The mean positive bias in the SMOS brightness temperatures can partly explain the observed dry bias in the SMOS L2 soil moisture products, that were found by dall'Amico (2012). A more pronounced overestimation of brightness temperatures would be necessary to explain it entirely. However, as the SMOS L1c data processing described in Sect. 2.3 uses stricter filtering techniques than the official SMOS processor, it is possible that the bias is decreased due to a more efficient filtering of RFI.

Figures 5–8 show both time series for the 20° and 40° look angles for both polarizations from April to October 2011 and Fig. 9 shows the scatter plots for the same comparisons. The error bars in Figs. 5–8 represent the standard deviation of the spatial (PROMET) and angular (SMOS) averaging of the data. The PROMET standard deviations are relatively large due to the high spatial resolution of PROMET which leads to very different land cover classes being averaged (e.g. bare soil and forest). The behaviour of the additional look angles, that were modelled, is analogue to the 20° and 40° comparisons (not shown). Due to orbit geometry there are less SMOS observations available for 20° than for 40°. For the angles 10° to 30° in the horizontal polarization the SMOS brightness temperatures are considerably lower than the modelled ones for the summer months between end of May and end of August. For the other months it is the other way round for all angles. For the angles 40° and 50° both data sets have comparable mean values for the summer months. For vertical polarization the behaviour is similar. PROMET standard deviations are smaller in the summer months from around mid of June until mid of August because the optical depth variations are smaller during this time as most crops have relatively high LAI values (compare Fig. 10). In August winter wheat is being harvested leaving bare soil fields while maize shows very high LAI values, therefore the standard deviation increases substantially. If the other two ISEA IDs in the Vils test site 2026586 and 2026587 are considered the big picture for the brightness temperature comparison is very similar but the performance concerning correlation, RMSE and regression tends to be lower (not shown), which is analogue to SMOS L2 soil moisture data performance.

The seasonal behaviour of SMOS is not as expected. The expected increase of brightness temperatures in summer is not at all visible due to a sharp drop in brightness temperatures at the beginning of June. This seasonal behaviour is not observable in

HESSD
9, 5389–5436, 2012

the model data that serve as input for L-MEB. Soil moisture modelling for example seems to work equally well before and after the drop (Fig. 3). The drop in brightness temperatures coincides roughly with the end of the pronounced drying period in April and May, but obviously the model data does not react as extreme to the increase in soil moisture as the SMOS data. Obviously there is either a pronounced problem with the brightness temperature data that may be linked to RFI or an unresolved radiative transfer problem. As it has been shown in Sect. 3.1 that the radiative transfer modelling works reliably, it is concluded that these problems are also related to RFI.

Of course this comparison involves the same approximations that are mentioned in the previous section that are related to the different geometries of the data sets compared. But due to the already demonstrated homogeneity of the Vils test site this is not expected to have a substantial impact.

For the interpretation of these results it is important to keep the uncertainties in mind that are related to the modelling approach. In Sect. 2.4.1 it is shown that the uncertainties of the land surface model have been assessed thoroughly and are considered to be small. Soil moisture, temperature and vegetation modelling work reliably. The radiative transfer modelling uncertainties are assessed in Sect. 2.4.2 in May and June 2010 in the study area. Under contrasting soil moisture, vegetation and temperature conditions it works reliably in most instances with brightness temperature RMSE values between 6 K and 9 K. Parts of these deviations can be explained with a known offset in the reference radiometer. The comparisons in this section show considerably larger deviations during the same time of year. As both results were obtained under similar conditions in the same area, the radiative transfer modelling uncertainties are considered to play a minor role here.

3.3 Analysis of SMOS optical depth Tau

As the vegetation optical depth plays an important role in the SMOS soil moisture retrieval and could prove to be a valuable source of information about vegetation characteristics, it has been analysed for the year 2011. Figure 10 shows the time series of the comparison between modelled and SMOS L2 optical depth for low vegetation for April to October 2011 at the central ISEA ID in the Vils test site. Error bars indicate the DQX value for SMOS and the standard deviation of the averaging for PROMET. Analogue to the brightness temperatures, the PROMET standard deviations are relatively high due to the high spatial resolution of PROMET. The correlation coefficient for this comparison is 0.33 and the bias (SMOS-PROMET) 0.18. The comparison looks similar when the two additional ISEA IDs in the Vils test site are considered. SMOS values are generally too high although the correlation coefficients differ for the IDs (correlation coefficient: −0.27 and 0.03 for ID 2026587 and 2026586, respectively; bias: 0.10 and 0.13 for ID 2026587 and 2026586, respectively) (not shown). The seasonal behaviour is different from ID to ID, while some peaks are constant in time. The seasonal pattern of vegetation optical depth for a temperate region with a high percentage of crops consists of an increase from spring until summer during the crop growth phase and a decrease in fall during ripening and harvesting. This is not clearly apparent in the SMOS data. The increase in April and May seems to be captured as well as a decrease in October but the variability of SMOS optical depth appears very high with several peaks throughout the year compared to typical vegetation phenology. The mean value of 0.40 is relatively high when compared to model simulations and typical values found in literature that range between maximum values of 0.3 and 0.4 for low vegetation (Wigneron et al., 2007; Saleh et al., 2007). A visual comparison to MODIS NDVI data from (ORNL-DAAC, 2012) did not deliver any similarity with SMOS optical depth either. It does not seem to have a physical meaning which was also found by (Jackson et al., 2012) in the US. The high variability, the unclear seasonal pattern and the high values of optical depth could indicate that SMOS optical depth also depends on other parameters than vegetation. Possibly RFI in the brightness temperatures or parameters in the radiative transfer modelling that are compensated by Tau could play a role here.

To test whether there is a relationship between SMOS retrieved soil moisture and optical depth, both data sets were compared. Although a visual comparison of the time series does not allow any conclusions, the scatter plot (Fig. 11) shows a clear

HESSD
9, 5389–5436, 2012

relationship with a correlation coefficient of 0.65, which is similar for the other Vils IDs. This is the largest correlation coefficient determined in the whole study and per se surprising as soil moisture and optical depth are considered independent variables in our area. This clearly indicates a retrieval problem. Modelled soil moisture and optical depth show no significant correlation ($R = 0.053$) for the same comparison.

4 Conclusion and outlook

The land surface model PROMET and the radiative transfer model L-MEB have been coupled and used as a tool for the analysis of SMOS passive microwave satellite observations. The coupled models have been shown to work well in determining the L-band microwave emission under varying soil moisture, vegetation and temperature conditions during the SMOS Validation Campaign 2010. Their output has been compared to ground data and airborne L-band brightness temperature measurements. A considerable part of the observed brightness temperature RMSE, which is around 6 K–9 K, is attributed to a known bias in the airborne L-band measurements. Therefore the L-MEB parameterizations used in this study are considered reliable enough to be used for SMOS validation activities. However, a further optimisation under local conditions may still be possible. A known uncertainty factor that should further be investigated is the brightness temperature behaviour shortly after precipitation events.

SMOS L1c brightness temperature data have been compared to airborne brightness temperatures on two days during the SMOS Validation Campaign 2010 from which no reliable conclusions can be drawn due to the small data set.

Next, an extensive comparison of SMOS L1c with modelled brightness temperatures from April to October 2011 was performed in the Vils test site. SMOS L1c brightness temperatures do not show the expected seasonal behaviour and are positively biased. SMOS L1c data do not perform better than L2 soil moisture data in the Vils test site, which could have pointed towards a pure retrieval problem. It is concluded that RFI is responsible for most of the observed problems in the SMOS L2 soil moisture product.

HESSD
9, 5389–5436, 2012

This is consistent with the observed dry bias in the SMOS L2 soil moisture products which can be related to RFI as stated by (Oliva et al., 2012). It is confirmed that the brightness temperature data from the lower SMOS look angles are less reliable which has also been reported by (Bircher et al., 2012). This information could be used to improve the brightness temperature data filtering before the SMOS soil moisture retrieval.

SMOS L2 optical depth values have been compared to modelled data using vegetation parameters from the dynamic vegetation model in PROMET. SMOS optical depth does not seem to be a reliable source of information about vegetation characteristics due to missing seasonal behaviour and very high values. This could originate from RFI or soil moisture retrieval problems. Indeed a strong correlation between SMOS L2 soil moisture and optical depth was found that was not expected ($R = 0.65$). This points clearly towards retrieval problems and should be further investigated.

As it has been shown that the radiative transfer modelling abilities of the coupled models are reliable in most instances under local conditions when compared to airborne data, it seems probable that RFI is responsible for most of the observed problems in the SMOS data. Therefore RFI mitigation efforts should be continued to improve SMOS data quality.

The clear improvement in SMOS L2 soil moisture performance from 2010 to 2011 that is shown by (dall'Amico et al., 2012a) and (dall'Amico, 2012) demonstrates that significant improvements in the performance of the SMOS satellite products are possible during the first years of such a mission. In other parts of the world, the SMOS L2 soil moisture product performs very well. (Jackson et al., 2012) e.g. state that the RMSE of the comparison between SMOS L2 soil moisture and measurements in four catchments in the US are $0.043\,\mathrm{m^3\,m^{-3}}$. This demonstrates that the SMOS soil moisture retrieval can work very reliably if there is no RFI. To study the potential origin of problems in the SMOS L2 soil moisture product, coupled land surface and radiative transfer models are helpful.

The value of coupled land surface and radiative transfer models for the validation and analysis of passive microwave remote sensing data has been shown in this study. The

HESSD
9, 5389–5436, 2012

models made an extensive SMOS data analysis possible that would have been limited to a few days of distributed ground and airborne data without them. Even though an extensive field campaign was conducted, hardly any conclusions could be drawn from this without the models.

In a next step the coupled models could be used for different soil moisture retrievals from SMOS L1c data to assess the potential of improvements in the SMOS L2 soil moisture product.

Acknowledgement. The SMOS Validation Campaign 2010 was organized and funded by the ESA with the indispensable contribution of the teams of the Aalto University and the Technical University of Denmark. The authors wish to acknowledge the contributions of the students of the University of Munich helping with the in situ measurements and the assistance given by Timo Gebhardt in the data processing. The authors would like to thank J.-P. Wigneron for making the model L-MEB available. The ELBARA instrument was kindly provided by ESA. Meteorological data and technical and logistical support in running the soil moisture stations were kindly provided by the Bavarian State Research Center for Agriculture, Department Meteorology (Mr. Kerscher), which is gratefully acknowledged. This work was supported by the German Federal Ministry of Economics and Technology through the German Aerospace Center (DLR, 50 EE 0731) which is gratefully acknowledged. Alexander Loew was supported by the Cluster of Excellence "CliSAP" (EXC177), University of Hamburg, funded through the German Science Foundation (DFG).

References

Albergel, C., Calvet, J.-C., de Rosnay, P., Balsamo, G., Wagner, W., Hasenauer, S., Naeimi, V., Martin, E., Bazile, E., Bouyssel, F., and Mahfouf, J.-F.: Cross-evaluation of modelled and remotely sensed surface soil moisture with in situ data in southwestern France, Hydrol. Earth Syst. Sci., 14, 2177–2191, doi:10.5194/hess-14-2177-2010, 2010.

Albergel, C., Zakharova, E., Calvet, J.-C., Zribi, M., Pardé, M., Wigneron, J.-P., Novello, N., Kerr, Y., Mialon, A., and Fritz, N.-E.-D.: A first assessment of the SMOS data in Southwestern France using in situ and airborne soil moisture estimates: the CAROLS airborne campaign, Remote Sens. Environ., 115, 2718–2728, doi:10.1016/j.rse.2011.06.012, 2011.

Albergel, C., de Rosnay, P., Gruhier, C., Muñoz-Sabater, J., Hasenauer, S., Isaksen, L., Kerr, Y., and Wagner, W.: Evaluation of remotely sensed and modelled soil moisture products using global ground-based in situ observations, Remote Sens. Environ., 118, 215–226, doi:10.1016/j.rse.2011.11.017, 2012.

Bach, H. and Mauser, W.: Methods and examples for remote sensing data assimilation in land surface process modeling, IEEE T. Geosci. Remote, 41, 1629–1637, 2003.

Bach, H., Braun, M., Lampart, G., and Mauser, W.: Use of remote sensing for hydrological parameterisation of Alpine catchments, Hydrol. Earth Syst. Sci., 7, 862–876, doi:10.5194/hess-7-862-2003, 2003.

Balling, J. E., Kristensen, S. S., Sobjaerg, S. S., and Skou, N.: Surveys and analysis of RFI in preparation for SMOS: results from airborne campaigns and first impressions from satellite data, IEEE T. Geosci. Remote, 49, 4821–4831, 2011.

Bartalis, Z., Wagner, W., Anderson, C., Bonekamp, H., Naeimi, V., and Hasenauer, S.: Validation of coarse resolution microwave soil moisture products, Int. Geosci. Remote Se., II-173–176, 2008.

Bircher, S., Balling, J. E., Skou, N., and Kerr, Y.: Validation of SMOS Brightness Temperatures During the HOBE Airborne Campaign, Western Denmark, IEEE T. Geosci. Remote, 50, 1468–1482, doi:10.1109/tgrs.2011.2170177, 2012.

Bolten, J. D., Crow, W. T., Xiwu, Z., Jackson, T. J., and Reynolds, C. A.: Evaluating the utility of remotely sensed soil moisture retrievals for operational agricultural drought monitoring, IEEE J. Sel. Top. Appl., 3, 57–66, 2010.

Brooks, R. and Corey, A.: Hydraulic properties of porous media, Tech. Rep., Hydrology Paper 3, Colorado State University, Fort Collins, Colorado, 1964.

BÜK 1000 Bodenübersichtskarte Deutschland 1 : 1 000 000: available at: http://www.bgr.bund.de/cln_006/nn_325414/DE/Themen/Boden/Produkte/Karten/BUEK_1000.html (last access date: 13 January 2008), 1997.

Crow, W. T., Ryu, D., and Famiglietti, J. S.: Upscaling of field-scale soil moisture measurements using distributed land surface modeling, Adv. Water Resourc., 28, 1–14, doi:10.1016/j.advwatres.2004.10.004, 2005.

dall'Amico, J.: Multiscale analysis of soil moisture using satellite and aircraft microwave remote sensing, in situ measurements and numerical modeling, Ph.D., Department for Geography, Ludwig Maximilians University, Munich, Germany, 2012.

dall'Amico, J. T., Schlenz, F., Loew, A., and Mauser, W.: First results of SMOS soil moisture validation in the Upper Danube catchment, IEEE T. Geosci. Remote, 50, 1507–1516, doi:10.1109/tgrs.2011.2171496, 2012a.

dall'Amico, J. T., Schlenz, F., Loew, A., Mauser,W., Kainulainen, J., Balling, J., and Bouzinac, C.: The SMOS Validation Campaign 2010 in the Upper Danube catchment: a data set for studies of soil moisture, brightness temperature and their spatial variability over a heterogeneous land surface, IEEE T. Geosci. Remote, accepted, 2012b.

Delwart, S., Bouzinac, C., Wursteisen, P., Berger, M., Drinkwater, M., Martin-Neira, M., and Kerr, Y. H.: SMOS validation and the COSMOS campaigns, IEEE T. Geosci. Remote, 46, 695–704, 2008.

Dirmeyer, P. A.: Using a global soil wetness dataset to improve seasonal climate simulation, J. Climate, 13, 2900–2922, doi:10.1175/1520-0442(2000)013¡2900:UAGSWD¿2.0.CO;2, 2000.

Dorigo, W. A., Wagner, W., Hohensinn, R., Hahn, S., Paulik, C., Xaver, A., Gruber, A., Drusch, M., Mecklenburg, S., van Oevelen, P., Robock, A., and Jackson, T.: The International Soil Moisture Network: a data hosting facility for global in situ soil moisture measurements, Hydrol. Earth Syst. Sci., 15, 1675–1698, doi:10.5194/hess-15-1675-2011, 2011.

Entekhabi, D., Asrar, G. R., Betts, A. K., Beven, K. J., Bras, R. L., Duffy, C. J., Dunne, T., Koster, R. D., Lettenmaier, D. P., Mclaughlin, D. B., Shuttleworth, W. J., Van Genuchten, M. T., Wei, M.-Y., and Wood, E. F.: An agenda for land-surface hydrology research and a call for the second international hydrological decade, B. Am. Meteorol. Soc., 80, 2043–2057, 1999.

ESA: Mission Objectives and Scientific Requirements of the Soil Moisture and Ocean Salinity (SMOS) Mission, Version 5, European Space Agency (ESA), 2002.

Grant, J. P., Wigneron, J. P., Van de Griend, A. A., Kruszewski, A., Søbjærg, S. S., and Skou, N.: A field experiment on microwave forest radiometry: L-band signal behaviour for varying conditions of surface wetness, Remote Sens. Environ., 109, 10–19, doi:10.1016/j.rse.2006.12.001, 2007.

Gruhier, C., de Rosnay, P., Hasenauer, S., Holmes, T., de Jeu, R., Kerr, Y., Mougin, E., Njoku, E., Timouk, F., Wagner, W., and Zribi, M.: Soil moisture active and passive microwave products: intercomparison and evaluation over a Sahelian site, Hydrol. Earth Syst. Sci., 14, 141–156, doi:10.5194/hess-14-141-2010, 2010.

Hank, T.: A Biophysically Based Coupled Model Approach for the Assessment of Canopy Processes under Climate Change Conditions, Phd, Department for Geography, Ludwig Maximilians University, Munich, Germany, 2008.

Hornbuckle, B. K., Rowlandson, T. L., Patton, J. C., and Bramer, L. M.: How is the angular signature of SMOS brightness temperature different in the morning and evening?, Int. Geosci. Remote Se., 3125–3128, 2011.

Jackson, T. J., Bindlish, R., Cosh, M. H., Zhao, T., Starks, P. J., Bosch, D. D., Seyfried, M., Moran, M. S., Goodrich, D. C., Kerr, Y. H., and Leroux, D.: Validation of Soil Moisture and Ocean Salinity (SMOS) soil moisture over watershed networks in the US, IEEE T. Geosci. Remote, 50, 1530–1543, doi:10.1109/tgrs.2011.2168533, 2012.

Juglea, S., Kerr, Y., Mialon, A., Wigneron, J.-P., Lopez-Baeza, E., Cano, A., Albitar, A., Millan-Scheiding, C., Carmen Antolin, M., and Delwart, S.: Modelling soil moisture at SMOS scale by use of a SVAT model over the Valencia Anchor Station, Hydrol. Earth Syst. Sci., 14, 831–846, doi:10.5194/hess-14-831-2010, 2010.

Kerr, Y. H., Waldteufel, P., Wigneron, J. P., Delwart, S., Cabot, F., Boutin, J., Escorihuela, M. J., Font, J., Reul, N., Gruhier, C., Juglea, S. E., Drinkwater, M. R., Hahne, A., Martín-Neira, M., and Mecklenburg, S.: The SMOS mission: new tool for monitoring key elements of the global water cycle, Proc. IEEE, 98, 666–687, 2010.

Kerr, Y. H., Waldteufel, P., Richaume, P., Davenport, P., Ferrazzoli, P., and Wigneron, J.-P.: SMOS level 2 processor soil moisture algorithm theoretical basis document (ATBD) V 3.5, CBSA, UoR, TV and INRA, Toulouse, 2011.

Loew, A.: Impact of surface heterogeneity on surface soil moisture retrievals from passive microwave data at the regional scale: the Upper Danube case, Remote Sens. Environ., 112, 231–248, doi:10.1016/j.rse.2007.04.009, 2008.

Loew, A. and Schlenz, F.: A dynamic approach for evaluating coarse scale satellite soil moisture products, Hydrol. Earth Syst. Sci., 15, 75–90, doi:10.5194/hess-15-75-2011, 2011.

Loew, A., Ludwig, R., and Mauser, W.: Derivation of surface soil moisture from ENVISAT ASAR wide swath and image mode data in agricultural areas, IEEE T. Geosci. Remote, 44, 889–899, 2006.

Ludwig, R. and Mauser, W.: Modelling catchment hydrology within a GIS based SVAT-model framework, Hydrol. Earth Syst. Sci., 4, 239–249, doi:10.5194/hess-4-239-2000, 2000.

Ludwig, R., Mauser, W., Niemeyer, S., Colgan, A., Stolz, R., Escher-Vetter, H., Kuhn, M., Reichstein, M., Tenhunen, J., Kraus, A., Ludwig, M., Barth, M., and Hennicker, R.: Web-based

modelling of energy, water and matter fluxes to support decision making in mesoscale catchments – the integrative perspective of GLOWA-Danube, Phys. Chem. Earth, 28, 621–634, 2003.
Mauser, W. and Bach, H.: PROMET – Large scale distributed hydrological modelling to study the impact of climate change on the water flows of mountain watersheds, J. Hydrol., 376, 362–377, 2009.
Mauser, W. and Schädlich, S.: Modelling the spatial distribution of evapotranspiration on different scales using remote sensing data, J. Hydrol., 212–213, 250–267, doi:10.1016/s0022-1694(98)00228-5, 1998.
Miralles, D. G., Crow, W. T., and Cosh, M. H.: Estimating spatial sampling errors in coarse-scale soil moisture estimates derived from point-scale observations, J. Hydrometeorol., 11, 1423–1429, doi:10.1175/2010JHM1285.1, 2010.
Montzka, C., Bogena, H., Weihermueller, L., Jonard, F., Dimitrov, M., Bouzinac, C., Kainulainen, J., Balling, J. E., Vanderborght, J., and Vereecken, H.: Radio brightness validation on different spatial scales during the SMOS validation campaign 2010 in the Rur catchment, Germany, Int. Geosci. Remote Se., 3760–3763, 2011.
Muerth, M.: A Soil Temperature and Energy Balance Model for Integrated Assessment of Global Change Impacts at the regional scale, Phd, Department for Geography, Ludwig Maximilians University, Munich, Germany, 2008.
Oliva, R., Daganzo-Eusebio, E., Kerr, Y. H., Mecklenburg, S., Nieto, S., Richaume, P., and Gruhier, C.: SMOS radio frequency interference scenario: status and actions taken to improve the RFI environment in the 1400-1427-MHz passive band, IEEE T. Geosci. Remote, 50, 1427–1439, doi:10.1109/tgrs.2012.2182775, 2012.
Panciera, R., Walker, J. P., and Merlin, O.: Improved understanding of soil surface roughness parameterization for L-band passive microwave soil moisture retrieval, IEEE Geosci. Remote S., 6, 625–629, 2009.
Parrens, M., Zakharova, E., Lafont, S., Calvet, J.-C., Kerr, Y., Wagner, W., and Wigneron, J.-P.: Comparing soil moisture retrievals from SMOS and ASCAT over France, Hydrol. Earth Syst. Sci., 16, 423–440, doi:10.5194/hess-16-423-2012, 2012.
Pauwels, V. R. N., Timmermans, W., and Loew, A.: Comparison of the estimated water and energy budgets of a large winter wheat field during AgriSAR 2006 by multiple sensors and models, J. Hydrol., 349, 425–440, doi:10.1016/j.jhydrol.2007.11.016, 2008.

HESSD
9, 5389–5436, 2012
Analysis of SMOS data with coupled models
F. Schlenz et al.

Philip, J.: The theory of infiltration: 1. the infiltration equation and its solution, Soil Sci., 83, 345–357, 1957.
Prigent, C., Aires, F., Rossow, W. B., and Robock, A.: Sensitivity of satellite microwave and infrared observations to soil moisture at a global scale: relationship of satellite observations to in situ soil moisture measurements, J. Geophys. Res., 110, D07110, doi:10.1029/2004jd005087, 2005.
Probeck, M., Ludwig, R., and Mauser, W.: Fusion of NOAA-AVHRR imagery and geographical information system techniques to derive subscale land cover information for the upper Danube watershed, Hydrol. Process., 19, 2407–2418, doi:10.1002/hyp.5892, 2005.
Rowlandson, T. L., Hornbuckle, B. K., Bramer, L. M., Patton, J. C., and Logsdon, S. D.: Comparisons of evening and morning SMOS passes over the Midwest United States, IEEE T. Geosci. Remote, 50, 1544–1555, doi:10.1109/tgrs.2011.2178158, 2012.
Saleh, K., Wigneron, J. P., Waldteufel, P., de Rosnay, P., Schwank, M., Calvet, J. C., and Kerr, Y. H.: Estimates of surface soil moisture under grass covers using L-band radiometry, Remote Sens. Environ., 109, 42–53, doi:10.1016/j.rse.2006.12.002, 2007.
Saleh, K., Kerr, Y. H., Richaume, P., Escorihuela, M. J., Panciera, R., Delwart, S., Boulet, G., Maisongrande, P., Walker, J. P., Wursteisen, P., and Wigneron, J. P.: Soil moisture retrievals at L-band using a two-step inversion approach (COSMOS/NAFE'05 experiment), Remote Sens. Environ., 113, 1304–1312, doi:10.1016/j.rse.2009.02.013, 2009.
Schlenz, F., dall'Amico, J. T., Loew, A., and Mauser, W.: Uncertainty assessment of the SMOS validation in the Upper Danube Catchment, IEEE T. Geosci. Remote, 50, 1517–1529, doi:10.1109/tgrs.2011.2171694, 2012a.
Schlenz, F., Fallmann, J., Marzahn, P., Loew, A., and Mauser, W.: Characterization of rape field microwave emission and implications to surface soil moisture retrievals, Remote Sens., 4, 247–270, 2012b.
Schwank, M., Wiesmann, A., Werner, C., Mätzler, C., Weber, D., Murk, A., Völksch, I., and Wegmüller, U.: ELBARA II, an L-band radiometer system for soil moisture research, Sensors, 10, 584–612, 2009.
Skou, N., Misra, S., Balling, J. E., Kristensen, S. S., and Sobjaerg, S. S.: L-band RFI as experienced during airborne campaigns in preparation for SMOS, IEEE T. Geosci. Remote, 48, 1398–1407, 2010.

HESSD
9, 5389–5436, 2012

Analysis of SMOS data with coupled models

F. Schlenz et al.

Strasser, G., Schneider, K., and Mauser, W.: The use of ERS SAR data derived soil moisture distributions for SVAT-model validation, Int. Geosci. Remote Se., 4, 1921–1923, doi:10.1109/igarss.1999.774987, 1999.

Strasser, U. and Mauser, W.: Modelling the spatial and temporal variations of the water balance for the Weser catchment 1965–1994, J. Hydrol., 254, 199–214, doi:10.1016/s0022-1694(01)00492-9, 2001.

Wigneron, J. P., Kerr, Y., Waldteufel, P., Saleh, K., Escorihuela, M. J., Richaume, P., Ferrazzoli, P., de Rosnay, P., Gurney, R., Calvet, J. C., Grant, J. P., Guglielmetti, M., Hornbuckle, B., Mätzler, C., Pellarin, T., and Schwank, M.: L-band Microwave Emission of the Biosphere (L-MEB) model: description and calibration against experimental data sets over crop fields, Remote Sens. Environ., 107, 639–655, doi:10.1016/j.rse.2006.10.014, 2007.

HESSD

9, 5389–5436, 2012

Analysis of SMOS data with coupled models

F. Schlenz et al.

HESSD
9, 5389–5436, 2012

Analysis of SMOS data with coupled models

F. Schlenz et al.

Table 1. The land cover specific L-MEB parameters used for the radiative transfer modelling.

	H_R	Q_R	NRh/NRv	tt$h$/tt$v$	$\omega h/\omega v$	b'	b''
Bare soil	0.1	0	0/ – 1	1/1	0/0	0	0
Crops general	0.15	0	0/ – 1	1/1	0/0	0.05	0
Wheat	0.1	0	0/ – 1	1/8	0/0	0.035	0
Corn	0.6	0	0/ – 1	2/1	0.05/0.05	0.05	0
Grass	1.3–1.13*SM	0	1/0	1/1	0/0.05	0.04	0.03
Coniferous	1.2	0	1.8/2	0.9/0.8	0.07/0.07	τNAD = 0.65	0
Deciduous	1.	0	1/2	0.6/0.5	0.07/0.07	τNAD =1	0
Rape	0.93	0	0/ – 1	1/1	0/0	0.09	0.08

HESSD

9, 5389–5436, 2012

Analysis of SMOS data with coupled models

F. Schlenz et al.

Table 2. The statistics for the comparison of SMOS L1c and modelled brightness temperature for different look angles for the central ISEA ID in the Vils test site (2027099) in 2011.

Look angle	R [–]	RMSE [K]	Gain [–]	Offset (SMOS-PROMET) [K]	Mean (STDV) SMOS [K]	Mean (STDV) PROMET [K]	N
TBH10	0.17	12.09	0.14	−4.13	245.24 (7.86)	249.37 (8.97)	35
TBH20	0.13	13.14	0.13	1.0	248.97 (10.24)	247.97 (9.47)	67
TBH30	0.29	12.46	0.27	4.04	249.68 (9.79)	245.64 (10.39)	99
TBH40	0.3	17.69	0.27	11.58	254.08 (10.82)	242.50 (11.91)	130
TBH50	0.41	21.82	0.33	17.94	256.85 (11.05)	238.91 (14.20)	77
TBV10	0.29	10.50	0.25	2.73	252.97 (8.21)	250.24 (8.65)	35
TBV20	0.1	12.71	0.11	2.35	255.66 (9.93)	253.31 (8.60)	67
TBV30	0.3	11.38	0.38	1.05	259.03 (10.63)	257.98 (8.40)	99
TBV40	0.39	10.99	0.56	0.94	264.69 (11.30)	263.75 (7.83)	130
TBV50	0.36	12.77	0.66	−5.52	264.57 (12.32)	270.09 (6.77)	77

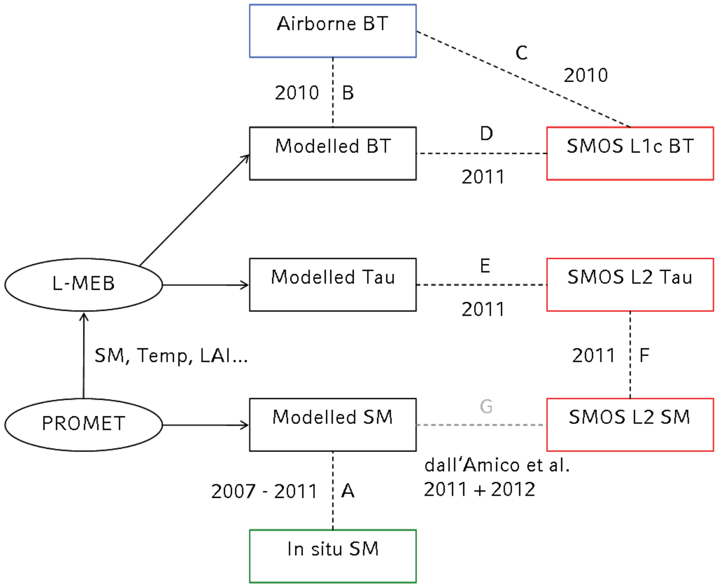

Fig. 1. A flowchart illustrating the different data sets (boxes) and comparisons (dashed lines) in this paper. Black boxes depict modelled data sets provided by the models PROMET and L-MEB, red boxes represent SMOS data, the blue box airborne data and the green box in situ data. The comparisons consist of: (A) land surface model validation with in situ soil moisture (SM) from the years 2007–2011; (B) radiative transfer model validation with airborne EMIRAD brightness temperatures (BT) during the SMOS Validation Campaign 2010; (C) analysis of SMOS L1c brightness temperatures with EMIRAD data during the SMOS Validation Campaign 2010; (D) analysis of SMOS L1c with modelled brightness temperatures throughout the vegetation period 2011; (E) analysis of SMOS L2 optical depth (Tau) with modelled optical depth Tau throughout the vegetation period 2011; (F) comparison of SMOS L2 optical depth and SMOS L2 soil moisture throughout the vegetation period 2011; The analysis of SMOS L2 soil moisture with modelled soil moisture (G) has already been performed by dall'Amico et al. (2012a) and dall'Amico (2012) and is not subject of this paper.

HESSD
9, 5389–5436, 2012

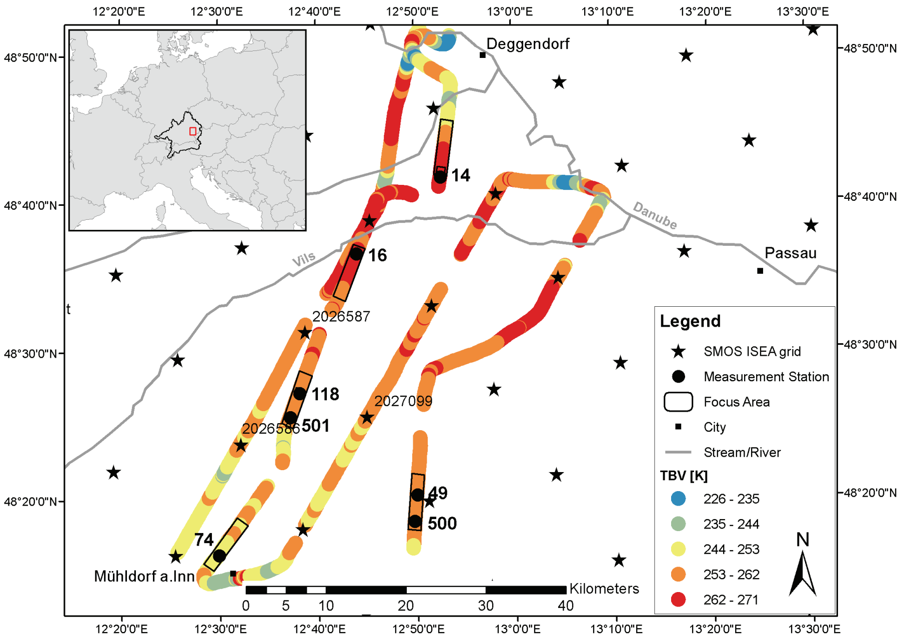

Fig. 2. The Vils test site with focus areas, soil moisture measuring stations, SMOS ISEA IDs and EMIRAD TBV data from 12 June 2010. The small overview map in the upper left corner shows the location of the Upper Danube Catchment (black) and the Vils test site (red) in Central Europe.

HESSD

9, 5389–5436, 2012

Analysis of SMOS data with coupled models

F. Schlenz et al.

Title Page
Abstract | Introduction
Conclusions | References
Tables | Figures
◀| |▶
◀ ▶
Back | Close
Full Screen / Esc
Printer-friendly Version
Interactive Discussion

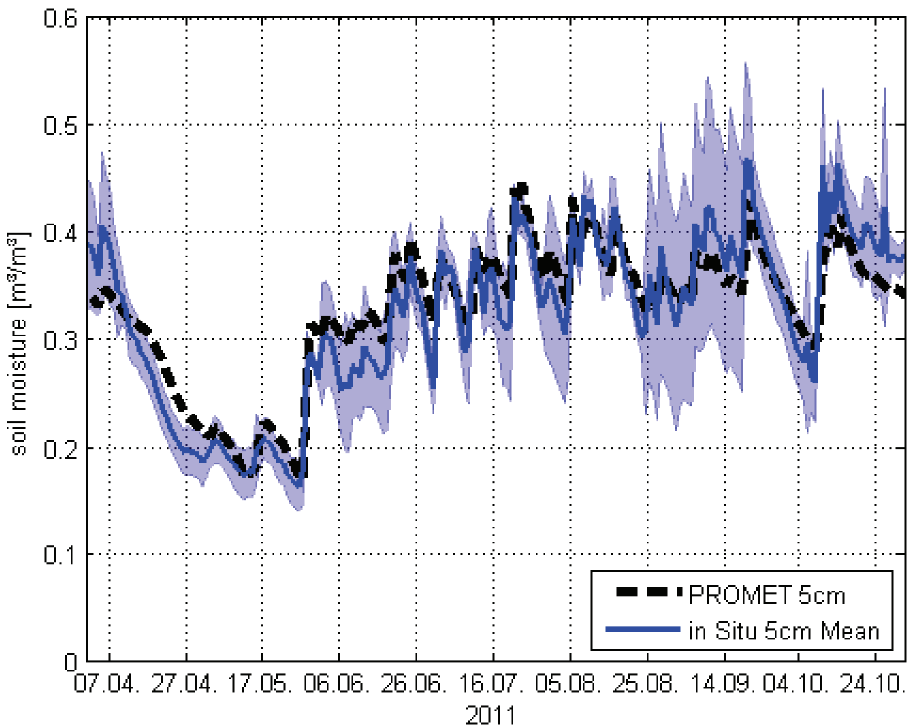

Fig. 3. A comparison of modelled and measured soil moisture in 5 cm depth from April to October 2011. Shown are the mean values of the five soil moisture stations that are within 20 km radius of the SMOS ID 2027099. ± one standard deviation are indicated for the in situ data.

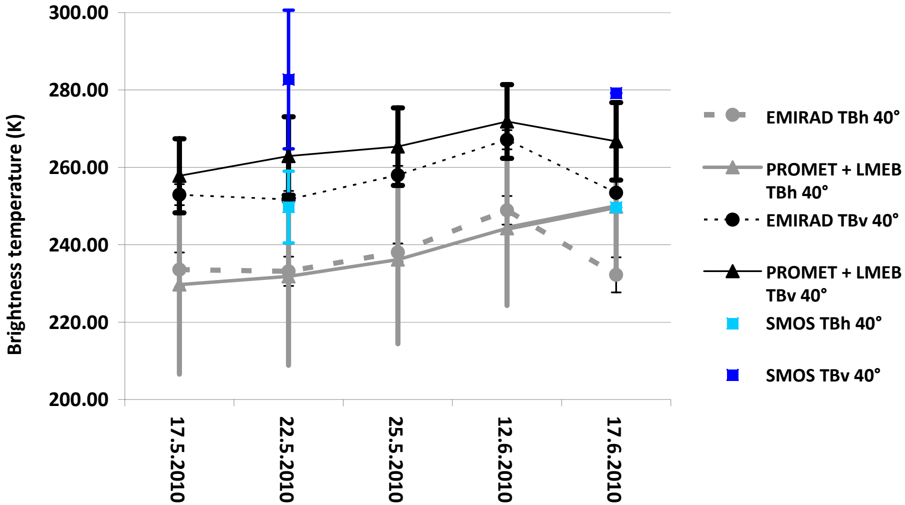

Fig. 4. A comparison of modelled (triangles) and measured (EMIRAD, circles) 40° brightness temperatures on the five campaign days of the SMOS Validation Campaign 2010 based on the central ISEA grid point in the Vils test site (2027099). For completion the SMOS L1c brightness temperatures for 40° are also plotted for the two days they are available (squares). All data sets are valid roughly for 06:00 a.m. local time.

HESSD
9, 5389–5436, 2012

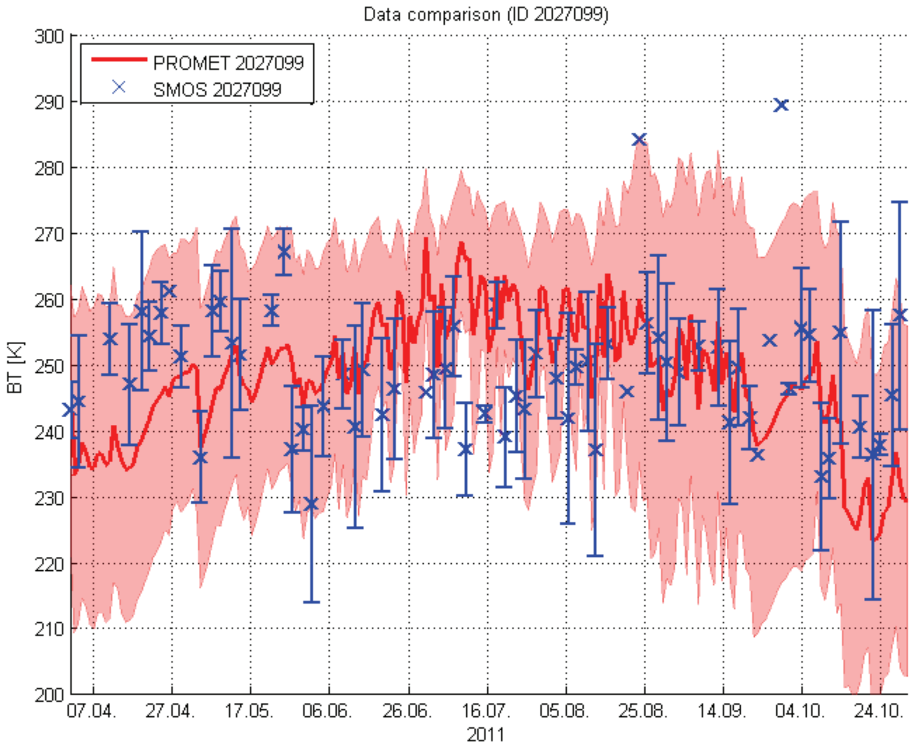

Fig. 5. The time series of modelled and SMOS L1c brightness temperatures for April to October 2011 for the 20° look angle and horizontal polarization for the central ISEA grid point in the Vils test site. Error bars indicate ± one standard deviation for angular (SMOS) and spatial (model) averaging.

HESSD
9, 5389–5436, 2012

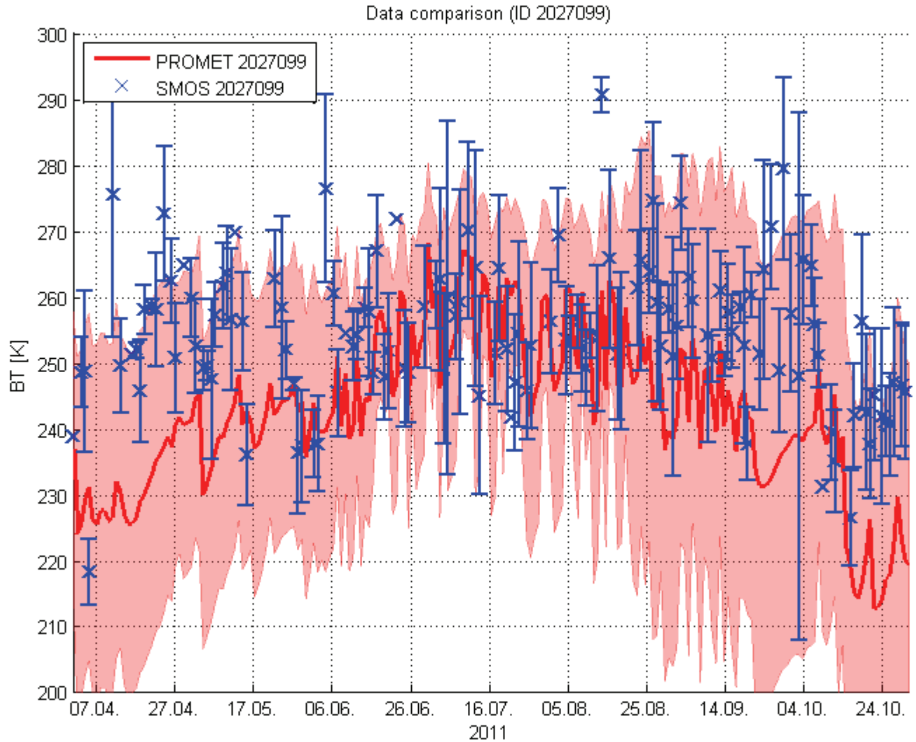

Fig. 6. The time series of modelled and SMOS L1c brightness temperatures for April to October 2011 for the 40° look angle and horizontal polarization for the central ISEA grid point in the Vils test site. Error bars indicate ± one standard deviation for angular (SMOS) and spatial (model) averaging.

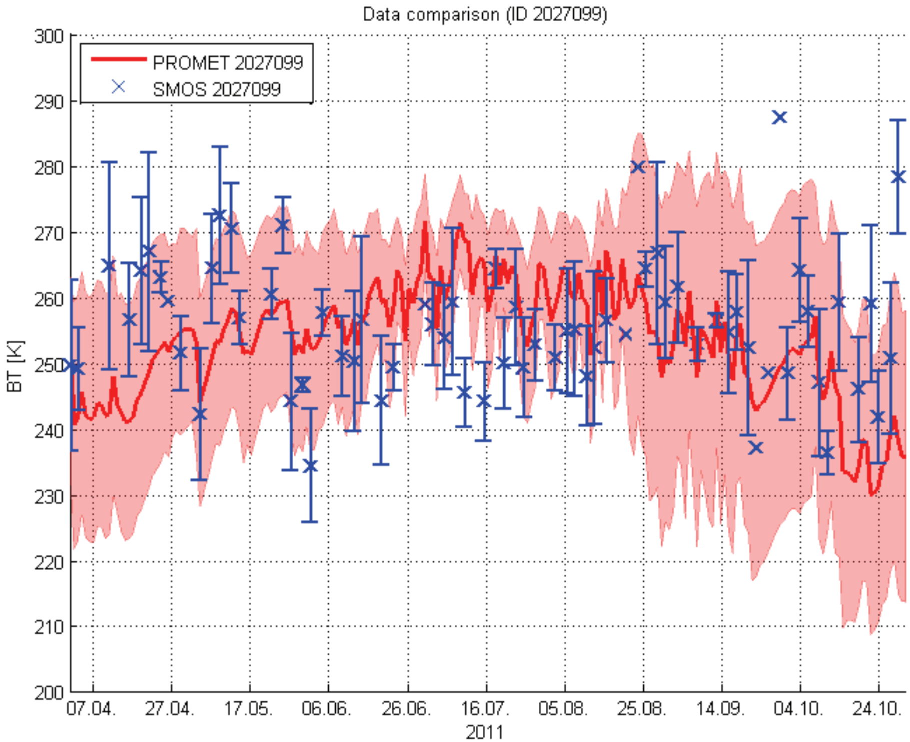

Fig. 7. The time series of modelled and SMOS L1c brightness temperatures for April to October 2011 for the 20° look angle and vertical polarization for the central ISEA grid point in the Vils test site. Error bars indicate ± one standard deviation for angular (SMOS) and spatial (model) averaging.

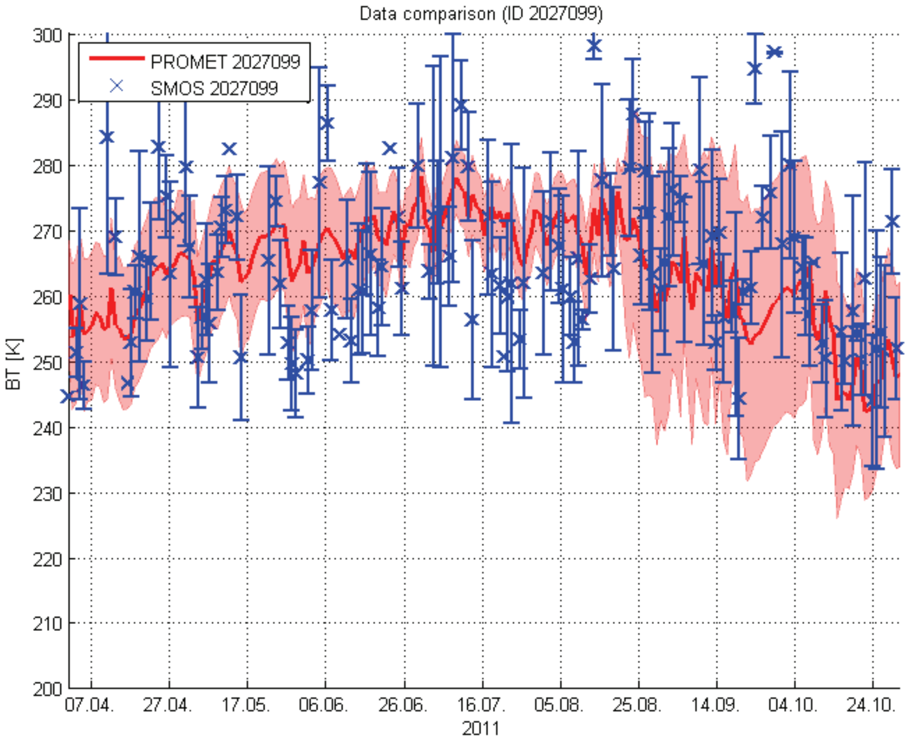

Fig. 8. The time series of modelled and SMOS L1c brightness temperatures for April to October 2011 for the 40° look angle and vertical polarization for the central ISEA grid point in the Vils test site. Error bars indicate ± one standard deviation for angular (SMOS) and spatial (model) averaging.

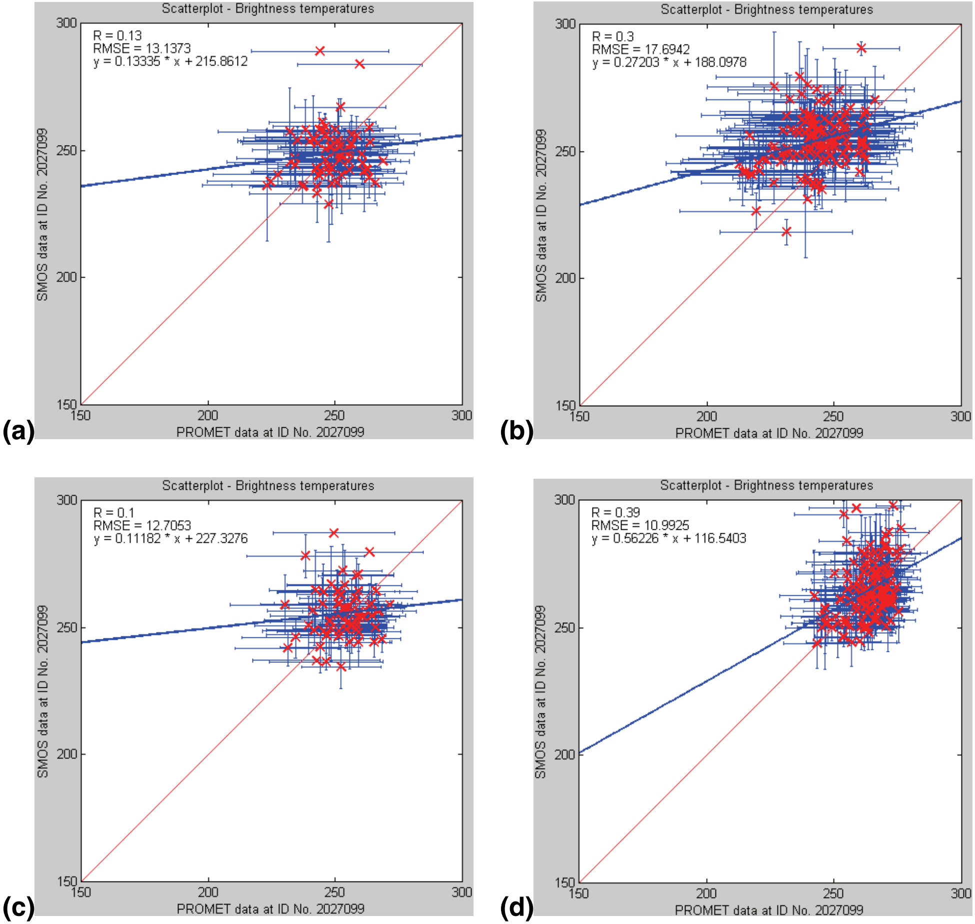

Fig. 9. Scatter plots for the comparison of modelled vs. SMOS L1c brightness temperatures for the look angles H20° **(a)**, H40° **(b)**, V20° **(c)**, V40° **(d)**.

HESSD
9, 5389–5436, 2012

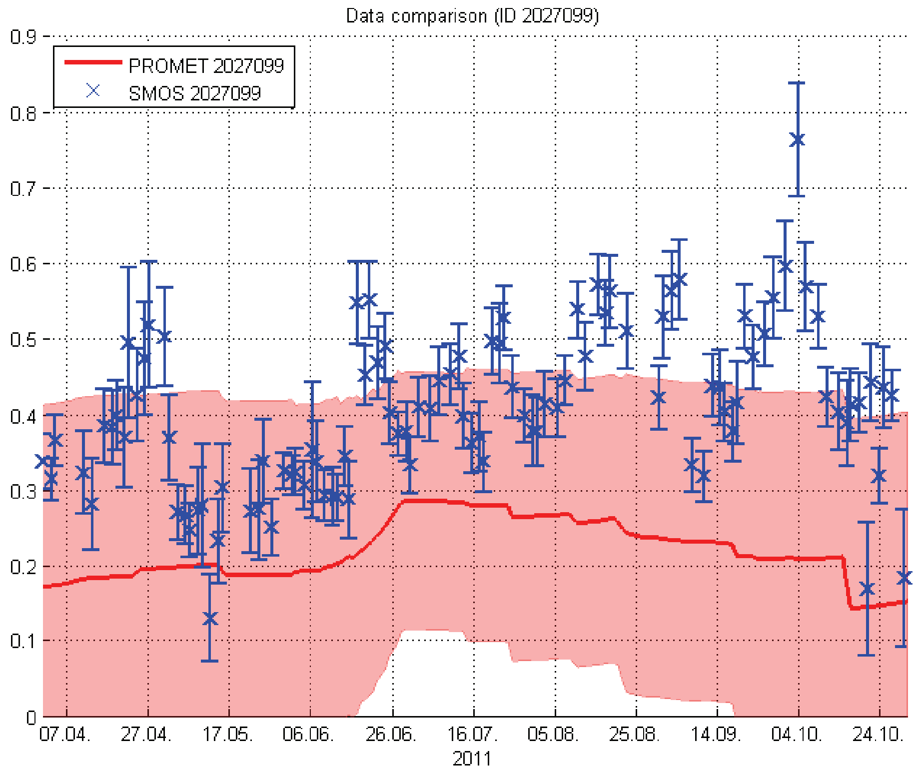

Fig. 10. A comparison between modelled (red) and SMOS L2 optical depth (blue) for the central ISEA ID in the Vils test site. Both values are valid for the nominal land use class (low vegetation). Error bars indicate ± the DQX value for SMOS and the standard deviation for the spatial averaging for PROMET.

HESSD
9, 5389–5436, 2012

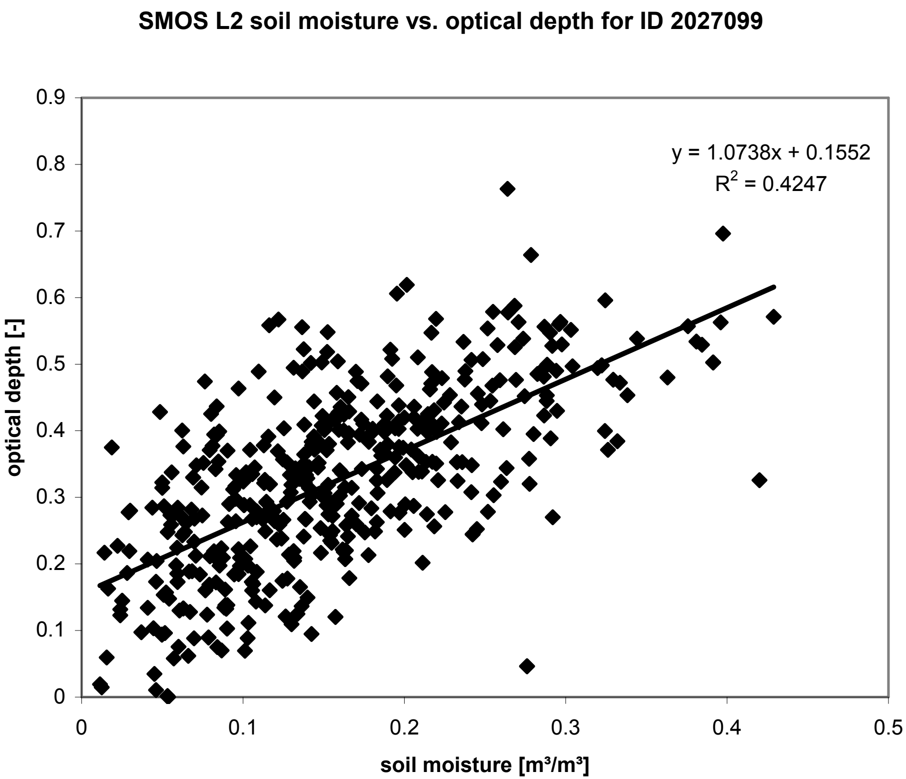

Fig. 11. Scatter plot for the comparison between SMOS L2 soil moisture and optical depth for the ID 2027099.

HESSD
9, 5389–5436, 2012

Analysis of SMOS data with coupled models

F. Schlenz et al.